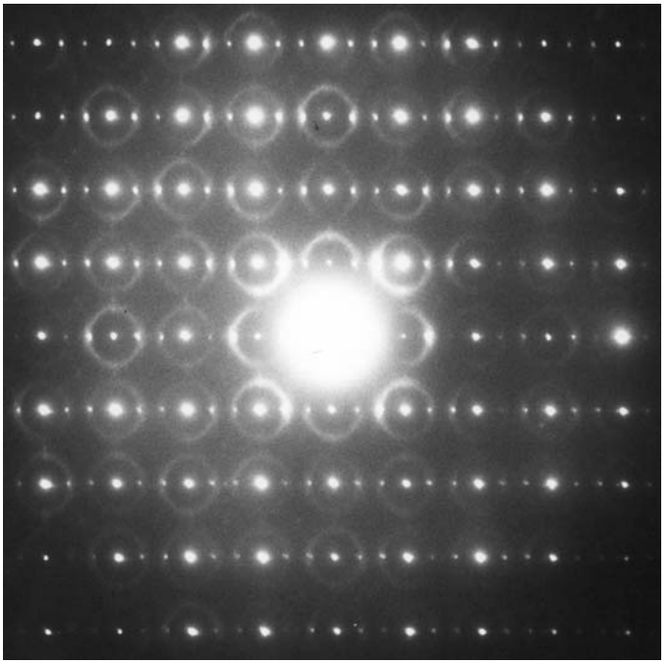

Fig. 4.3.1.2. Electron-diffraction pattern from a disordered crystal of $17Nb_2O_5{\cdot}48WO_3$ close to the [001] orientation of the tetragonal tungsten-bronze-type structure (Iijima & Cowley, 1977).

(1) Diffuse-scattering distributions can be recorded from very small specimen regions, a few nm in diameter and a few nm thick. The diameter of the specimen area may be varied readily up to several μm.

(2) Diffraction information on defects or disorder may be correlated with high-resolution electron-microscope imaging of the same specimen area [see Section 4.3.8 in *IT* C (2004)].

(3) The electron-diffraction pattern approximates to a planar section of reciprocal space, so that complicated configurations of diffuse scattering may be readily visualized (see Fig. 4.3.1.2).

(4) Dynamical effects may be exploited to obtain information about localization of sources of the diffuse scattering within the unit cell.

These experimental and theoretical aspects of electron diffraction have influenced the ways in which it has been applied in studies of diffuse scattering.

In general, we may distinguish three different approaches to the interpretation of diffuse scattering:

(*a*) The crystallographic way, in which the Patterson- or correlation-function representation of the local order is emphasized, *e.g.* by use of short-range-order parameters.

(*b*) The physical model in terms of excitations. These are usually described in reciprocal (momentum) space: phonons, plasmons *etc.*

(*c*) Structure models in direct space. These must be derived by trial or by chemical considerations of bonds, coordinates *etc.*

Owing to the difficulties of separating the different components in the diffuse scattering, most work on diffuse scattering of electrons has followed one or both of the two last approaches, although Patterson-type interpretation, based upon kinematical scattering including some dynamical corrections, has also been tried.

4.3.2. Inelastic scattering

In the kinematical approximation, a general expression which includes inelastic scattering can be written in the form quoted by Van Hove (1954)

$$I(\mathbf{u}, \nu) = \frac{m^3}{2^2h^6}\frac{k}{k_o} \times W(\mathbf{u}) \sum P_{n_o} \sum_{\eta} \sum_{j=1}^{Z} |\langle n_o| \exp\{2\pi i \mathbf{u}\cdot\mathbf{R}_j\}|n\rangle|^2 \times \delta\left(\nu + \frac{E_n - E_{n_o}}{h}\right) \quad (4.3.2.1)$$

for the intensity of scattering as function of energy transfer and momentum transfer from a system of Z identical particles, $\mathbf{R}_j$. Here m and h have their usual meanings; k_o and k, E_{n_o} and E_n are wavevectors and energies before and after the scattering between object states n_o and n; P_{n_o} are weights of the initial states; $W(\mathbf{u})$ is a form factor (squared) for the individual particle.

In equation (4.3.2.1), $\mathbf{u}$ is essentially momentum transfer. When the energy transfer is small ($\Delta E/E \ll \theta$), we can still write $|\mathbf{u}| = 2\sin\theta/\lambda$, then the sum over final states n is readily performed and an expression of the Waller–Hartree type is obtained for the total inelastic scattering as a function of angle:

$$I_{\text{inel}}(\mathbf{u}) \propto \frac{S}{u^4},$$

where

$$S(u) = Z - \sum_{j=1}^{Z} |f_{jj}(u)|^2 - \sum_{j\neq k}^{Z}\sum^{Z} |f_{jk}(u)|^2, \quad (4.3.2.2)$$

and where the one-electron f's for Hartree–Fock orbitals, $f_{jk}(\mathbf{u}) = \langle j|\exp(2\pi i\mathbf{u}\cdot\mathbf{r})|k\rangle$, have been calculated by Freeman (1959, 1960) for atoms up to $Z = 30$. The last sum is over electrons with the same spin only.

The Waller–Hartree formula may be a very good approximation for Compton scattering of X-rays, where most of the scattering occurs at high angles and multiple scattering is no problem. With electrons, it has several deficiencies. It does not take into account the electronic structure of the solid, which is most important at low values of u. It does not include the energy distribution of the scattering. It does not give a finite cross section at zero angle, if u is interpreted as an angle. In order to remedy this, we should go back to equation (4.3.1.2) and decompose $\mathbf{u}$ into two components, one tangential part which is associated with angle in the usual way and one normal component along the beam direction, u_n, which may be related to the excitation energy $\Delta E = E_n - E_{n_o}$ by the expression $u_n = \Delta E_k/2E$. This will introduce a factor $1/(u^2 + u_n^2)$ in the intensity at small angles, often written as $1/(\theta^2 + \theta_E^2)$, with ΔE estimated from ionization energies *etc.* (Strictly speaking, ΔE is not a constant, not even for scattering from one shell. It is a weighted average which will vary with u.)

Calculations beyond this simple adjustment of the Waller–Hartree-type expression are few. Plasmon scattering has been treated on the basis of a nearly free electron model by Ferrel (1957):

$$\frac{\mathrm{d}^2\sigma}{\mathrm{d}(\Delta E)\,\mathrm{d}\Omega} = (1/\pi^2 a_H m v^2 N)(-\mathrm{Im}\{1/\varepsilon\})/(\theta^2 + \theta_E^2), \quad (4.3.2.3)$$

where m, v are relativistic mass and velocity of the incident electron, N is the density of the valence electrons and $\varepsilon(\Delta E, \theta)$ their dielectric constant. Upon integration over ΔE:

$$\frac{\mathrm{d}\sigma}{\mathrm{d}\Omega} = \frac{E_p}{2\pi a_H mvN}[1/(\theta^2 + \theta_E^2)G(\theta, \theta_c)], \qquad (4.3.2.4)$$

where $G(\theta, \theta_c)$ takes account of the cut-off angle Θ_c. Inner-shell excitations have been studied because of their importance to spectroscopy. The most realistic calculations may be those of Leapman *et al.* (1980) where one-electron wavefunctions are determined for the excited states in order to obtain 'generalized oscillator strengths' which may then be used to modify equation (4.3.1.2).

At high energies and high momentum transfer, the scattering will approach that of free electrons, *i.e.* a maximum at the so-called Bethe ridge, $E = h^2u^2/2m$.

A complete and detailed picture of inelastic scattering of electrons as a function of energy and angle (or scattering variable) is lacking, and may possibly be the least known area of diffraction by solids. It is further complicated by the dynamical scattering, which involves the incident and diffracted electrons and also the ejected atomic electron (see *e.g.* Maslen & Rossouw, 1984*a*,*b*).

4.3.3. Kinematical and pseudo-kinematical scattering

Kinematical expressions for TDS or defect and disorder scattering according to equation (4.3.1.3) can be obtained by inserting the appropriate atomic scattering factors in place of the X-ray scattering factors in Chapter 4.1. The complications introduced by dynamical diffraction are considerable (see Section 4.3.4). In the most general case, a complete specification of the disordered structure may be needed. However, for thin specimens, approximate treatments of the deviations from kinematical scattering may lead to relatively simple forms. Two such cases are treated in this section, both relying on the small-angle nature of electron scattering. The first is based upon the phase-object approximation, which applies to small angles and thin specimens.

The amplitude at the exit surface of a specimen can always be written as a sum of a periodic and a nonperiodic part, and may in analogy with the kinematical case [equation (4.3.1.1)] be written

$$\psi(\mathbf{r}) = \bar{\psi}(\mathbf{r}) + \Delta\psi(\mathbf{r}), \qquad (4.3.3.1)$$

where $\mathbf{r}$ is a vector in two dimensions. The intensities can be separated in the same way [*cf.* equation (4.3.1.3)].

When the phase-object approximation applies [Section 2.5.2.4(*b*)]

$$\begin{aligned}\psi(\mathbf{r}) &= \exp\{-i\sigma\varphi(\mathbf{r})\} \\ &= \exp\{-i\sigma\bar{\varphi}(\mathbf{r})\}[1 - i\sigma\Delta\varphi(\mathbf{r}) - \ldots]. \end{aligned} \qquad (4.3.3.2)$$

Then the Bragg reflections are given by Fourier transform of the periodic part, *viz*:

$$\langle\exp\{-i\sigma\varphi(\mathbf{r})\}\rangle = \exp\{-i\sigma\bar{\varphi}(\mathbf{r})\}\exp\left\{-\tfrac{1}{2}\sigma^2\langle\Delta\varphi^2(\mathbf{r})\rangle\right\}; \qquad (4.3.3.3)$$

note that an absorption function is introduced.

The diffuse scattering derives from

$$-i\sigma\Delta\varphi(\mathbf{r})\exp\{-i\sigma\bar{\varphi}(\mathbf{r})\}, \qquad (4.3.3.4)$$

so that

$$I_d(\mathbf{u}) = \sigma^2|\Delta\Phi(\mathbf{u}) * \Phi_{av}(\mathbf{u})|^2. \qquad (4.3.3.5)$$

Thus, the kinematical diffuse-scattering amplitude is convoluted with the amplitude function for the average structure, *i.e.* the set of sharp Bragg beams. When the direct beam, $\Phi_{av}(0)$, is relatively strong, the kinematical diffuse scattering will be modified to only a limited extent by convolution with the Bragg reflections. To the extent that the diffuse scattering is periodic in reciprocal space, the effect will be to modify the intensity by a slowly varying function. Thus the shapes of local diffuse maxima will not be greatly affected.

The electron-microscope image contrast derived from the diffuse scattering will be obtained by inserting equation (4.3.3.4) in the appropriate intensity expressions of Section 4.3.8 of *IT* C (2004).

Another approach may be used for extended crystal defects in thin films, *e.g.* faults normal or near-normal to the film surface. Often, an average periodic structure may not readily be defined, as in the case of a set of incommensurate stacking faults. Kinematically, the projection of the structure in the simplest case may be described by convoluting the projection of a unit-cell structure with a nonperiodic set of delta functions which constitute a distribution function:

$$\varphi(\mathbf{r}) = \varphi_0(\mathbf{r}) * \sum_n \delta(\mathbf{r} - \mathbf{r}_n) = \varphi_0(\mathbf{r}) * \mathrm{d}(\mathbf{r}). \qquad (4.3.3.6)$$

Then the diffraction-pattern intensity is

$$I(\mathbf{u}) = |\Phi_0(\mathbf{u})|^2|D(\mathbf{u})|^2. \qquad (4.3.3.7)$$

Here, $\Phi_0(\mathbf{u})$ is the scattering amplitude of the unit whereas the function $|D(\mathbf{u})|^2$, where $D(\mathbf{u}) = \mathscr{F}\{d(\mathbf{r})\}$, gives the configuration of spots, streaks or other diffraction maxima corresponding to the faulted structure (see *e.g.* Marks, 1985).

In the projection (column) approximation to dynamical scattering, the wavefunction at the exit surface may be given by an expression identical to (4.3.3.6), but with a wavefunction, $\psi_0(\mathbf{r})$, for the unit in place of the projected potential, $\varphi_0(\mathbf{r})$.

An intensity expression of the same form as (4.3.3.7) then applies, with a dynamical scattering amplitude Ψ_0 for the scattering unit substituted for the kinematical amplitude Φ_0.

$$I(\mathbf{u}) = |\Psi_0(\mathbf{u})|^2|D(\mathbf{u})|^2, \qquad (4.3.3.8)$$

which in the simplest case describes a diffraction pattern with the same features as in the kinematical case. Note that $\Psi_0(\mathbf{u})$ may have different symmetries when the incident beam is tilted away from a zone axis, leading to diffuse streaks *etc.* appearing also in positions where the kinematical diffuse scattering is zero. More complicated cases have been considered by Cowley (1976*a*) who applied this type of analysis to the case of nonperiodic faulting in magnesium fluorogermanate (Cowley, 1976*b*).

4.3.4. Dynamical scattering: Bragg scattering effects

The distribution of diffuse scattering is modified by higher-order terms in essentially two ways: Bragg scattering of the incident and diffuse beams or multiple diffuse scattering, or by a combination.

Theoretical treatment of the Bragg scattering effects in diffuse scattering has been given by many authors, starting with Kainuma's (1955) work on Kikuchi-line contrast (Howie, 1963; Fujimoto & Kainuma, 1963; Gjønnes, 1966; Rez *et al.*, 1977; Maslen & Rossouw, 1984*a*,*b*; Wang, 1995; Allen *et al.*, 1997). Mathematical formalism may vary but the physical pictures and